AJNR

Diffusion-Weighted Imaging of Brain Metastasis from Lung Cancer: Correlation of MRI Parameters with the Histologic Type and Gene Mutation Status

W.S. Jung, C.H. Park, C.-K. Hong, S.H. Suh and S.J. Ahn

AJNR Am J Neuroradiol 2018, 39 (2) 273-279
doi: https://doi.org/10.3174/ajnr.A5516
http://www.ajnr.org/content/39/2/273

Diffusion-Weighted Imaging of Brain Metastasis from Lung Cancer: Correlation of MRI Parameters with the Histologic Type and Gene Mutation Status

W.S. Jung, C.H. Park, C.-K. Hong, S.H. Suh, and S.J. Ahn

ABSTRACT

BACKGROUND AND PURPOSE: Development of noninvasive imaging biomarkers indicating the histology and the gene mutation status of brain metastasis from lung cancer is important. We aimed to investigate diffusion-weighted imaging parameters as predictors of the histology and gene mutations of brain metastasis from lung cancer.

MATERIALS AND METHODS: DWI data for 74 patients with brain metastasis from lung cancer were retrospectively reviewed. The patients were first grouped according to the primary tumor histology (adenocarcinoma, small-cell lung cancer, squamous cell carcinoma), and those with adenocarcinoma were further divided into *epidermal growth factor receptor* (*EFGR*) mutation–positive and wild type groups. Sex; age; number, size, and location of brain metastasis; DWI visual scores; the minimum ADC; and the normalized ADC ratio were compared among groups using χ^2 and ANOVA. Multiple logistic regression analysis was performed to determine independent predictors of the *EGFR* mutation.

RESULTS: The minimum ADC was lower in the small-cell lung cancer group than in the other 2 groups, though the difference was not significant. Furthermore, minimum ADC and the normalized ADC ratio were significantly lower in the *EGFR* mutation–positive group than in the wild type group ($P = .021$ and .014, respectively). Multivariate analysis revealed that minimum ADC and the normalized ADC ratio were independently associated with the *EGFR* mutation status ($P = .028$ and .021, respectively).

CONCLUSIONS: Our results suggest that DWI parameters (minimum ADC and normalized ADC ratio) for the solid components of brain metastasis from lung cancer are not correlated with their histology, whereas they can predict the *EGFR* mutation status in brain metastasis from lung adenocarcinoma.

ABBREVIATIONS: ADC_{min} = minimum ADC; BM = brain metastasis; *EGFR* = *epidermal growth factor receptor*; nADC = normalized ADC; NSCLC = non-small-cell lung cancer; TKI = tyrosine kinase inhibitor

Lung cancer is one of the leading causes of cancer-related deaths in East Asia and the most frequent site of origin for brain metastasis (BM).[1-4] Despite advances in systemic therapy and improvement in survival rates for patients with advanced lung cancer, BM remains an important cause of morbidity and mortality.[1] Recently, many studies reported that compared with those with BM with wild type *epidermal growth factor receptor* (*EGFR*), patients with lung cancer with BM having *EGFR* mutations, particularly those with non-small-cell lung cancer (NSCLC), had improved survival due to higher response rates to whole-brain radiation therapy and specific chemotherapy medications such as *EGFR*-associated tyrosine kinase inhibitors (TKIs).[5-8]

Development of noninvasive imaging biomarkers indicating the gene mutation status of BM from lung cancer is important because they would provide clinicians with strong evidence for making clinical decisions, aid in the early initiation of specific chemotherapy for patients with gene mutations, and, consequently, contribute to an improved prognosis.[8]

Diffusion-weighted MR imaging of the brain is based on the differential diffusion rates or the Brownian motion of water. It is an essential technique for diagnosing acute infarction in the brain because of its ability to detect cytotoxic edema caused by altered water diffusion secondary to cellular damage. DWI is also widely used for the assessment of tumor pathology in the field of neuro-oncology.[9] Specifically, apparent diffusion coefficient values derived from DWI have been shown to correlate with tumor cellularity, glioma grade,

Received June 26, 2017; accepted after revision September 7.

From the Departments of Radiology (W.S.J., C.H.P., S.H.S., S.J.A.) and Neurosurgery (C.-K.H.), Gangnam Severance Hospital, Yonsei University, College of Medicine, Seoul, Korea; and Department of Radiology (W.S.J.), Ajou University School of Medicine, Suwon, Korea.

This study was supported by a faculty research grant from Yonsei University College of Medicine (6-2016-0111) and by a National Research Foundation of Korea (NRF) grant funded by the Korea government (MSIP) (No.2017R1C1B5014927). The funder had no role in study design, data collection and analysis, decision to publish, or preparation of the manuscript.

Please address correspondence to Sung Jun Ahn, MD, PhD, Department of Radiology, Gangnam Severance Hospital, Yonsei University, College of Medicine, 211 Eonju-ro, Gangnam-gu, Seoul 135-720, Korea; e-mail: aahng77@yuhs.ac

http://dx.doi.org/10.3174/ajnr.A5516

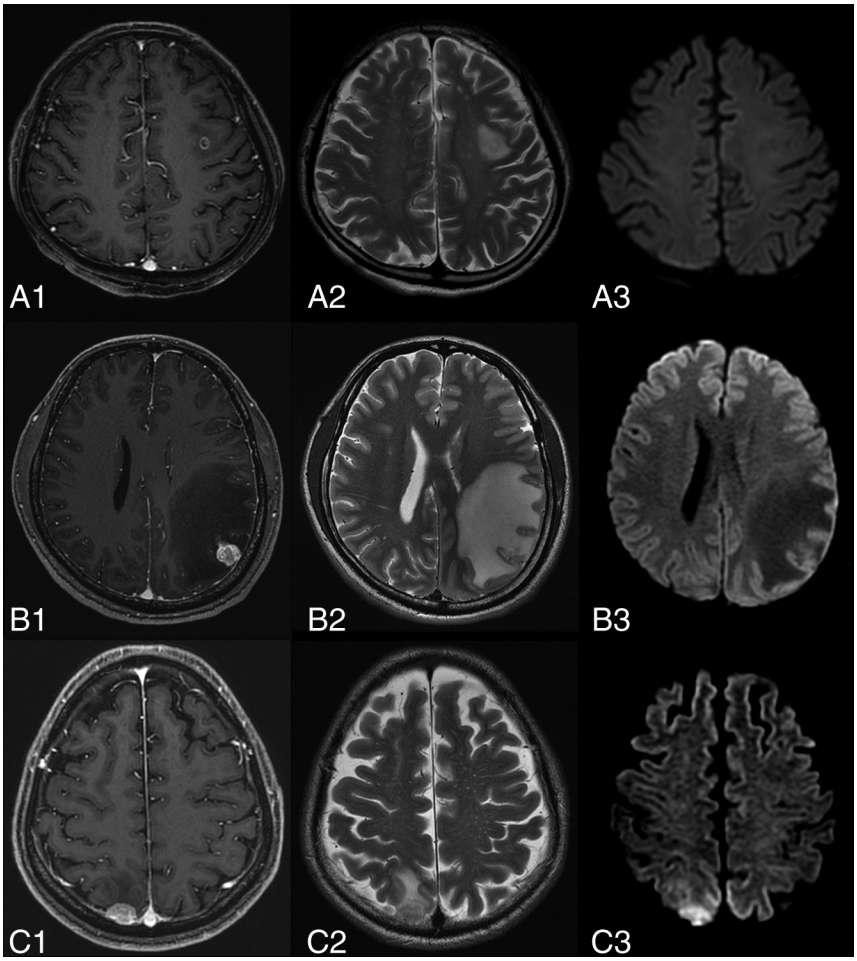

FIG 1. Representative MR images depicting visual scores based on diffusion-weighted imaging findings for brain metastasis from lung cancer. Contrast-enhanced T1-weighted images show an apparent enhanced tumor in the left frontal lobe (*A1*), left parietal lobe (*B1*), and right parietal lobe (*C1*). T2-weighted images (*A2*, *B2*, and *C2*) show varying degrees of peritumoral brain edema. *A3*, BM is not detectable on DWI (*A3*, score = 1). *B3* and *C3*, DWI images show iso-signal intensity (score = 2) and high signal intensity (score = 3), respectively, relative to the normal-appearing cortical gray matter.

and treatment response.[9-13] Moreover, recent studies have shown that DWI parameters may differentiate the histology of BM from lung cancer.[14,15] However, the association between DWI parameters and the gene mutation status has not been assessed for BM from lung cancer, to our knowledge.

We hypothesized that the molecular and genetic backgrounds of tumors affect signal intensity and ADC values of lung cancer BM on DWI. Therefore, we aimed to investigate DWI parameters as imaging biomarkers for prediction of the histologic type and gene mutation status of BM from lung cancer.

MATERIALS AND METHODS

Patient Population

We retrospectively reviewed data for 100 patients diagnosed with BM from lung cancer between January 2012 and April 2016. All patients had received a histopathologic diagnosis of lung cancer based on bronchoscopic, percutaneous needle-guided, or surgical biopsies and had undergone gene mutation studies. Accordingly, they were stratified into groups based on the histopathology of the lung cancer. Furthermore, patients with lung adenocarcinoma were divided according to the gene mutation status.

We excluded patients with the following conditions: MR imaging evidence of intratumoral hemorrhage ($n = 5$), lesions that were too small for the measurement of ADC values ($n = 12$), leptomeningeal seeding metastasis ($n = 6$), and a history of chemotherapy or radiation therapy for BM ($n = 3$). Eventually, 74 patients were included in this study. Approval for the use of clinical data was obtained from the internal review board of our institution (Gangnam Severance Hospital).

Pathology and EGFR Mutation Analysis of Lung Cancer

One experienced pathologist (Heae Surng Park, with 8 years of experience in pathology) evaluated the pathology and *EGFR* mutation status of the lung cancer. Genomic DNA was extracted from the lung cancer specimen, and *EGFR* tyrosine kinase exons 19, 20, and 21 and *V-Ki-ras2 Kirsten rat sarcoma viral oncogene homolog* (*Kras*) were amplified by a nested polymerase chain reaction using specific primers. Fluorescence in situ hybridization testing with *anaplastic lymphoma kinase* (*Alk*) break-apart probes was performed to detect rearrangements. The details of the sequencing procedure are described elsewhere.[16,17] The presence of *EGFR* mutations was determined by the presence of deletions within exons 19 and 20 and L858R point mutations in exon 21.

MR Imaging Protocol

All patients were imaged with a 3T clinical MR imaging device (Discovery MR750, GE Healthcare, Milwaukee, Wisconsin; Achieva, Philips Healthcare, Best, the Netherlands). Our MR imaging protocol for BM included routine T2-weighted fast-spin-echo sequences (TR/TE, 5414/96 ms), axial fluid-attenuated inversion recovery sequences (TR/TE/TI, 4000/80/2000 ms), axial diffusion-weighted echo-planar sequences (TR/TE, 8000/65.6 ms; slice thickness/intersection gap, 4/1 mm; matrix size, 160 × 160; FOV, 240 × 240 mm; 3 directions; b-value = 0 and 1000 s/mm^2), and contrast-enhanced 3D T1 fast-spoiled gradient-recalled sequences (TR/TE, 8.2/3.2 ms; flip angle, 12°; slice thickness, 1 mm; matrix size, 256 × 256; FOV, 220 × 220 mm). Intravenous gadolinium-based contrast agent was used at a dose of 0.1 mmol/kg body weight. ADC values were automatically calculated by the operating console of the MR imaging device and displayed as corresponding ADC maps.

Image Evaluation

Two experienced neuroradiologists (S.H.S., with 12 years of experience in neuroimaging, and S.J.A., with 6 years of experience in

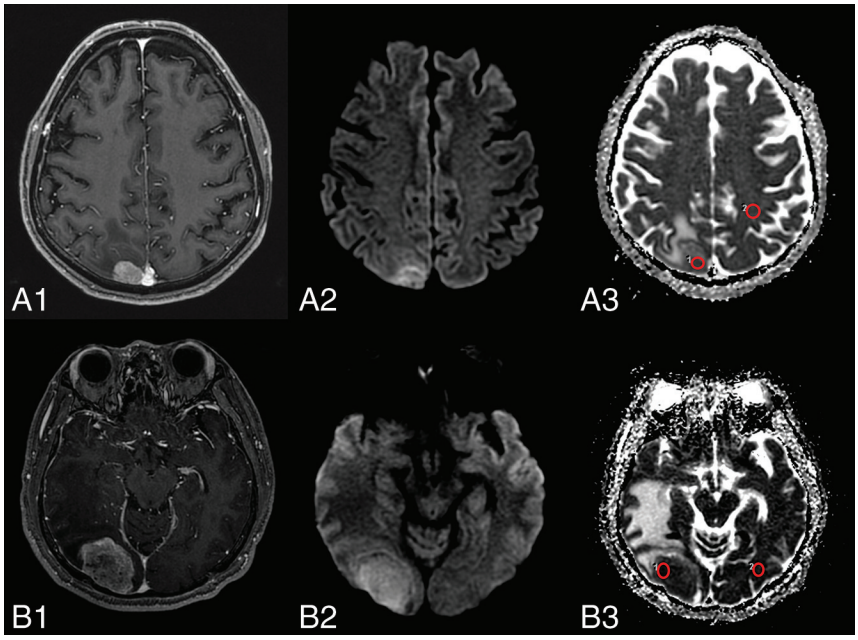

FIG 2. Representative images depicting the ROI within a tumor and the corresponding contralateral normal-appearing white matter for the calculation of apparent diffusion coefficient values for brain metastasis lesions stratified by the *EGFR* mutation status. *A1* and *B1*, Contrast-enhanced T1-weighted images show contrast enhancement of the metastasis. *A2* and *B2*, Diffusion-weighted images show mild-to-moderate high signal intensity in the contrast-enhanced areas. *A3* and *B3*, ADC map with ROIs within the tumor and corresponding contralateral normal-appearing white matter. *A1–A3*, Wild type *EGFR*. *B1–B3*, *EGFR* mutation–positive.

neuroimaging) visually assessed the signal intensity on DWI in areas corresponding to the enhanced portion of the lesions on contrast-enhanced T1-weighted images; both were blinded to the clinical and pathologic information. If there were multiple brain lesions, the largest one, which reflected DWI findings for most BM lesions, was selected as the target lesion to increase the accuracy of the measurement. The lesions on DWI were visually scored as follows: 1, negative findings on DWI; 2, isointense relative to the normal-appearing cortical gray matter; and 3, hyperintense relative to the normal-appearing cortical gray matter (Fig 1).

The study coordinator (W.S.J.) marked circular ROIs (each area, 20 mm^2) over the target lesion on the ADC map, avoiding cystic or necrotic parts. The minimum ADC (ADC_{min}) value was calculated from these ROIs. The same method was applied to a corresponding site in the contralateral white matter judged as normal on both contrast-enhanced T1- and T2-weighted images. Then, to assess the objective difference between the ADC value for the tumor and for the contralateral normal area, the normalized ADC (nADC) ratio was calculated as the ratio of the ADC_{min} of the tumor divided by the ADC_{min} of the corresponding contralateral white matter area (Fig 2).

Statistical Analysis

All statistical analyses were performed with the statistical software SAS, Version 9.2 (SAS Institute, Cary, North Carolina), and MedCalc for Windows, Version 12.7.0 (MedCalc Software, Mariakerke, Belgium). The χ^2 test and ANOVA were used to compare DWI visual scores, ADC_{min} values, the nADC ratio, the number and size of the BMs, and the presence of intratumoral necrosis or hemorrhage among the adenocarcinoma, squamous cell carcinoma, and small-cell lung carcinoma groups. Subgroup analysis according to the gene mutation status was also performed for the adenocarcinoma group. For multivariate analysis, a linear regression model was used to identify statistically significant variables. To investigate the interobserver reproducibility for DWI visual scores, we derived the intraclass correlation coefficient with a 2-way random model of absolute agreement.

RESULTS

Relationship between DWI Visual Scores and BM Histology and Mutation Status

In total, 74 patients (mean age, 64.19 ± 10.76 years; 50 men and 24 women) with BMs from lung cancer underwent DWI. Of these, 56 (75.67%) were diagnosed with adenocarcinoma (group 1); 11 (14.86%), with small-cell lung cancer (group 2); and 7 (9.45%), with squamous cell carcinoma (group 3). Of the 56 adenocarcinomas, 12 were poorly differentiated, 2 were well-differentiated, and 1 was moderately differentiated adenocarcinoma. For the remaining 41 cases of adenocarcinoma, detailed pathologic results were not available.

The 56 patients with adenocarcinoma were subdivided according to the status of mutations in *EGFR*, *Alk*, and *Kras*. In total, 55 patients had been examined for the *EGFR* mutation status, with 26 having *EGFR* mutations and 29 having wild type *EGFR*. Among the patients with *EGFR* mutations, 13, 4, and 9 had mutations in exons 19, 20, and 21, respectively. In addition, mutations were confirmed in 4 of 29 and 3 of 32 patients examined for *Alk* and *Kras* mutations, respectively.

Interobserver reproducibility for DWI visual scores was excellent (intraclass correlation coefficient, 0.972; 95% confidence interval, 0.955–0.982; $P < .001$). There was no significant difference in DWI visual scores among the 3 histology-based groups (Table 1) and between the 2 mutation-based groups (Table 2).

Relationship between ADC Values and Histologic Type

ADC_{min} and the nADC ratio were not significantly different among the small-cell lung cancer ($531.18 \pm 160.54 \times 10^{-6}$ mm^2/s and 0.88 ± 0.2, respectively), adenocarcinoma ($623.38 \pm 163.07 \times 10^{-6}$ mm^2/s and 1.04 ± 0.28, respectively), and squamous cell carcinoma ($682.14 \pm 182.07 \times 10^{-6}$ mm^2/s and 1.11 ± 0.28, respectively; $P = .131$ and 0.144) groups. Moreover, the location, size, and number of BMs and the presence of intratumoral hemorrhage or necrosis showed no significant differences among groups. The detailed patient characteristics are shown in Table 1.

Table 1: Characteristics of BM among primary lung cancer groups

	Total (n = 74)	Adenocarcinoma (n = 56)	Small-Cell Lung Cancer (n = 11)	Squamous Cell Carcinoma (n = 7)	P Value
DWI visual score		1.87 ± 0.76	2.27 ± 0.90	1.85 ± 0.69	.298
ADC_{min} ($\times 10^{-6} mm^2/s$)	615.23 ± 166.83	623.38 ± 163.07	531.18 ± 160.54	682.14 ± 182.07	.131
nADC ratio	1.02 ± 0.28	1.04 ± 0.28	0.88 ± 0.2	1.11 ± 0.28	.144
Age (yr)	64.19 ± 10.76	63.63 ± 11.15	68.09 ± 9.14	62.57 ± 9.73	.420
Male sex	50 (67.57)	36 (64.29)	9 (81.82)	5 (71.43)	.587
Site of BM					.545
Anterior circulation—dominant[a]	25 (33.78)	21 (37.5)	2 (18.18)	2 (28.57)	
Posterior circulation—dominant[b]	11 (14.86)	7 (12.5)	2 (18.18)	2 (28.57)	
Even distribution	38 (51.35)	28 (50)	7 (63.64)	3 (42.86)	
No. of BMs					.051
1	18 (24.32)	16 (28.57)	0 (0)	2 (28.57)	
1<BM<10	43 (58.11)	32 (57.14)	6 (54.55)	5 (71.43)	
≥10	13 (17.57)	8 (14.29)	5 (45.45)	0 (0)	
Target lesion size of BM					.367
<10 mm	31 (41.89)	22 (39.29)	7 (63.64)	2 (28.57)	
10 mm≤BM<30 mm	32 (43.24)	24 (42.86)	3 (27.27)	5 (71.43)	
≥30 mm	11 (14.86)	10 (17.86)	1 (9.09)	0 (0)	
Intratumoral necrosis	32 (43.24)	21 (37.5)	6 (54.55)	5 (71.43)	.160
Intratumoral hemorrhage	15 (20.27)	11 (19.64)	3 (27.27)	1 (14.29)	.882

[a] BMs mainly located in the frontal, parietal, and temporal lobes.
[b] BMs mainly located in the occipital lobes, cerebellum, and brain stem.

Table 2: Comparison of ADC_{min} values and normalized ADC ratio according to gene mutation status in adenocarcinoma group

	Wild Type	Mutation	P Value
EGFR	29 (52.7)	26 (47.3)	
DWI visual score	1.92 ± 0.77	1.87 ± 0.76	.179
ADC_{min} ($\times 10^{-6} mm^2/s$)	674.55 ± 182.78	575.85 ± 115.01	.021
nADC ratio	1.13 ± 0.32	0.95 ± 0.19	.014
Alk	25 (86.2)	4 (13.8)	
DWI visual score	1.96 ± 0.79	2 ± 1.15	.930
ADC_{min} ($\times 10^{-6} mm^2/s$)	583.8 ± 183.84	562 ± 159.12	.825
nADC ratio	1 ± 0.34	0.83 ± 0.19	.328
Kras	29 (90.6)	3 (9.4)	
DWI visual score	1.82 ± 0.77	2.33 ± 0.57	.274
ADC_{min} ($\times 10^{-6} mm^2/s$)	641.31 ± 168.32	631.45 ± 161.74	.310
nADC ratio	1.08 ± 0.31	1.08 ± 0.32	.926

Relationship between ADC Values and Gene Mutation Status

ADC_{min} was significantly lower in the *EGFR* mutation–positive group than in the wild type group (575.85 ± 115.01 × 10^{-6} mm^2/s versus 674.55 ± 182.78 × 10^{-6} mm^2/s, P = .021); similar results were obtained for the nADC ratio (0.95 ± 0.19 versus 1.13 ± 0.32, P = .014). However, there were no significant differences in the location, size, and number of BMs and the presence of necrosis or hemorrhage between groups (Table 2).

ADC_{min} and the nADC ratio also showed significant differences according to the following *EGFR* genotypes: exon 19 and/or 21 mutations (n = 22; 564.14 ± 109.25 × 10^{-6} mm^2/s and 0.93 ± 0.17, respectively), exon 20 mutations (n = 4; 640.25 ± 141.90 × 10^{-6} mm^2/s and 1.05 ± 0.28, respectively), and wild type *EGFR* (n = 29; 674.55 ± 182.78 × 10^{-6} mm^2/s and 1.13 ± 0.32, respectively; P = .049 and .038). A post hoc analysis showed that ADC_{min} and the nADC ratio were significantly lower in the exon 19 and/or 21 mutation group than in the wild type group (P = .039 and 0.029, respectively; Fig 3). There was no significant difference in the 2 parameters between the *Alk* mutation–positive and wild type groups and between the *Kras* mutation–positive and wild type groups (Table 2).

Multivariate logistic regression analysis revealed that ADC_{min} and the nADC ratio were independently associated with the *EGFR* mutation status (OR, 0.996; 95% CI, 0.992–1.000; P = .028; and OR, 0.064; 95% CI, 0.006–0.666; P = .021, respectively) after adjustment for sex; age; size, location, and number of BMs; presence of intratumoral necrosis or hemorrhage; and DWI visual scores. Specifically, ADC_{min} and the nADC ratio were significantly associated with exon 19 and/or 21 mutations (OR, 0.995; 95% CI, 0.991–0.999; P = .020; and OR, 0.044; 95% CI, 0.004–0.563; P = .016, respectively; Table 3).

DISCUSSION

In the present study, we tested the hypothesis that the signal intensity of BM from lung cancer on DWI may be expressed differently according to the genetic background of the lesion. Our results indicated a significant association of ADC_{min} and the nADC ratio with the *EGFR* mutation status and the location of the mutation. However, there was no association between the ADC parameters and the histologic type of the tumor.

A few previous studies have demonstrated opposing results for the relationship between the histologic type and DWI parameters for BM from lung cancer. Hayashida et al[14] evaluated 26 brain metastatic lesions in patients with primary lung cancer and reported that small- and large-cell neuroendocrine carcinomas showed high signal intensity on DWI. Thus, they concluded that signal intensity on DWI can predict the histology of metastases. However, Duygulu et al[15] evaluated 37 patients with BM from lung cancer and reported the absence of a correlation between

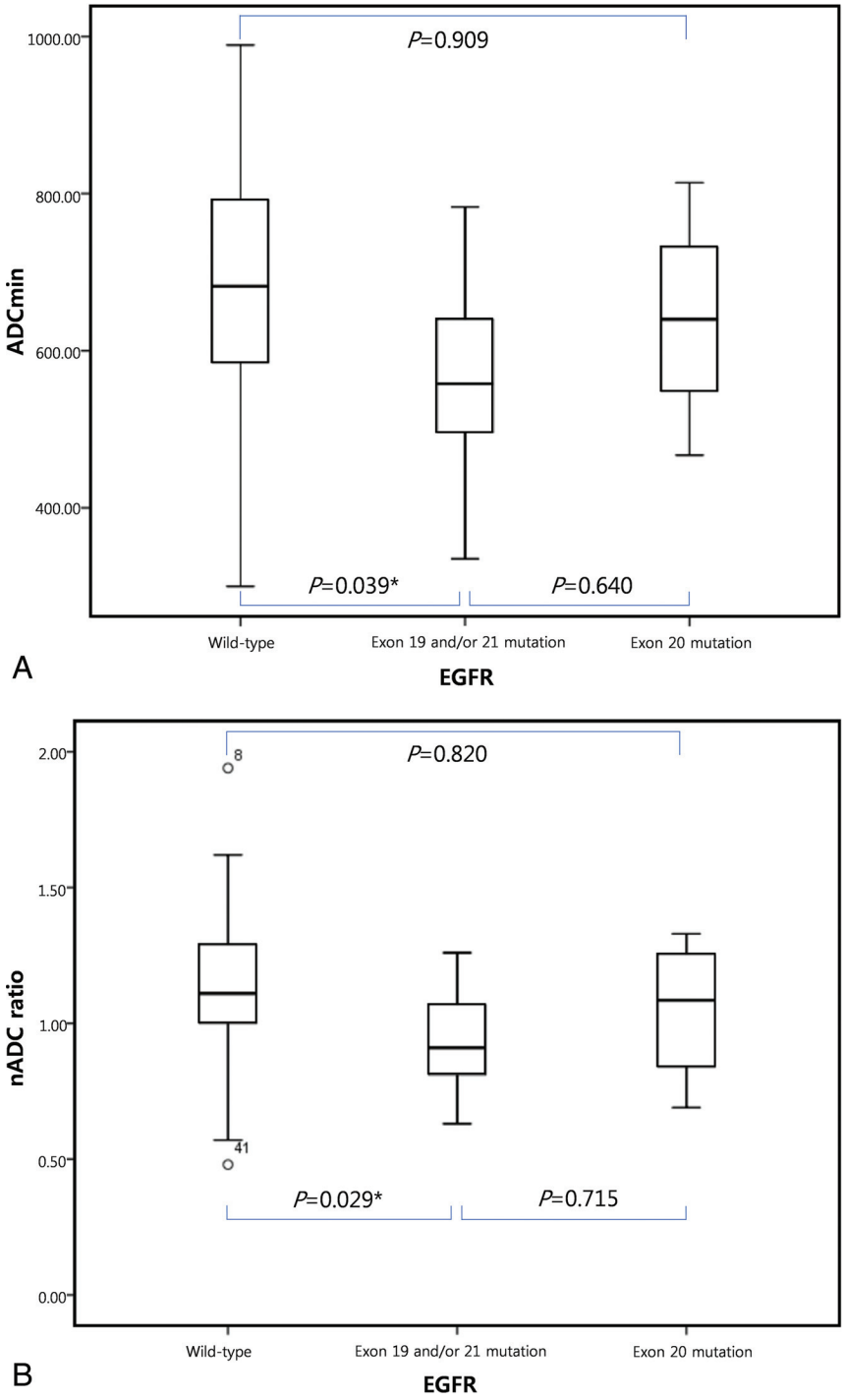

FIG 3. Boxplot for minimum apparent diffusion coefficient (*A*) and normalized ADC ratio (*B*) values for patients with lung adenocarcinoma with wild type *EGFR*, mutations in exon 19 and/or 21, and mutations in exon 20. *Asterisk* indicates statistically significant.

restricted diffusion on DWI and the primary pathology. In the present study, we also found no correlation between DWI parameters and BM histology; we believe our results are more reliable because of the large sample size compared with those in the previous studies. However, a nonsignificant trend existed for lower ADC_{min} and nADC in the small-cell lung cancer group, even compared with the adenocarcinoma *EGFR* mutation–positive group. In our results, most small-cell lung cancer cases (8/11) showed lower ADC values ($<600 \times 10^{-6}$ mm^2/s), while the minority (3/11) showed higher ADC values ($\geq 600 \times 10^{-6}$ mm^2/s). Two conflicting ADC values of small-cell lung cancer may explain the nonsignificant result of a lower ADC trend for small-cell lung cancer. We presume that there may be 2 different subtypes of small-cell lung cancer and would recommend further study.

EGFR is a transmembrane protein with cytoplasmic kinase activity that transduces important growth factor signaling from the extracellular milieu to the cell.[18] For patients with advanced NSCLC, initial therapy with a TKI can lead to substantial therapeutic improvement and may be considered as an alternative treatment for BM in the future.[8,17,19-21] Sensitive *EGFR* mutations are found in the first 4 exons (18–21) of the tyrosine kinase domain of *EGFR*, and the 2 major mutations are deletions in exon 19 and a single point mutation in exon 21 (L858R).[22-24] Identification of exon 19 or 21 mutation is also a useful tool for the prediction of response to treatment with TKI.[25-27] Also, several studies have demonstrated that the characteristics of BM are dependent on the *EGFR* genotype. The number of BM lesions was significantly higher in patients with *EGFR*-mutated NSCLC than in those with wild type NSCLC. Moreover, leptomeningeal metastases were more common in patients with *EGFR*-mutated NSCLC.[8] Tumors with exon 19 deletions reportedly showed a higher incidence of BM compared with tumors with exon 21 mutations.[28]

A previous study indicated that patients with NSCLC bearing exon 19 deletions exhibited a peculiar pattern of multiple, small brain metastases, similar to miliary BM.[29] Another study showed that brain metastases with exon 21 mutations were more common in the caudate, cerebellum, and temporal lobe compared with those with exon 19 deletions.[30] Other characteristic molecular changes of non-small-cell lung cancer are a *Kras* mutation and *Alk* rearrangement.[31,32] Patients who were *Alk*-positive and treated with the *Alk* TKI crizotinib in the second-line setting experienced improved progression-free survival compared with standard chemotherapy.[33] Patients with NSCLC with *Alk* rearrangements have improved survival outcome after radiation therapy for BMs.[34] On the contrary, there are currently no target therapy options for patients with the *Kras* mutation.

Table 3: Independent predictors of *EGFR* mutation status

Predictors	*EGFR* Mutation (Exon 19 + 20 + 21)		*EGFR* Mutation (Exon 19 + 21)	
	OR (95% CI)	*P* Value	OR (95% CI)	*P* Value
Female sex	1.630 (0.539–4.927)	.387	1.538 (0.483–4.898)	.466
Age, per 1-yr increase	0.975 (0.928–1.024)	.307	0.972 (0.923–1.024)	.282
Site of BM				
Anterior circulation–dominant[a]	Reference		Reference	
Posterior circulation–dominant[b]	0.750 (0.132–4.250)	.745	0.833 (0.145–4.781)	.837
Even distribution	0.867 (0.275–2.734)	.807	0.741 (0.222–2.471)	.625
No. of BM				
1	Reference		Reference	
1<BM<10	1.765 (0.491–6.337)	.383	1.765 (0.446–6.979)	.418
≥10	6.000 (0.873–41.214)	.068	7.500 (1.039–54.116)	.045
Target lesion size of BM				
<10 mm	Reference		Reference	
10 mm≤BM<30 mm	1.015 (0.318–3.243)	.979	0.923 (0.275–3.102)	.897
≥30 mm	1.500 (0.315–7.135)	.61	1.333 (0.260–6.828)	.729
Intratumoral necrosis	1.188 (0.395–3.569)	.759	0.887 (0.273–2.884)	.841
Intratumoral hemorrhage	1.440 (0.382–5.428)	.59	1.412 (0.353–5.649)	.625
Diffusion visual scoring	1.630 (0.680–2.601)	.199	1.514 (0.722–2.974)	.274
ADC_{min}	0.996 (0.992–1.000)	.028	0.995 (0.991–0.999)	.020
nADC ratio	0.064 (0.006–0.666)	.021	0.044 (0.004–0.563)	.016

[a] BMs mainly located in the frontal, parietal, and temporal lobes.
[b] BMs mainly located in the occipital lobes, cerebellum, and brain stem.

Gene expression analysis is based on invasive tissue sampling and can be associated with sampling errors; therefore, the development of imaging markers that reflect the gene mutation status is important.[35] Our findings demonstrated that low ADC values for BM from lung adenocarcinoma are associated with a high possibility of an *EGFR* mutation, particularly in exons 19 and 21. Such patients are expected to respond well to noninvasive TKI treatment, and clinicians can plan this treatment accordingly if the mutation status is known. Moreover, Huang et al[13] recently reported that ADC_{min} has the potential to predict and monitor the response of primary CNS lymphoma to chemotherapy. Therefore, through further study, we can apply serial ADC values to predict the response of BM from lung adenocarcinoma with *EGFR* mutations to TKI treatment.

Our study had several limitations. First, grades of lung cancer pathology (well, moderately, or poorly differentiated) in adenocarcinoma were not considered, which can affect the results of DWI parameters.[14] Second, the genetic testing was performed with samples obtained from the lungs because brain metastases were diagnosed using brain MR imaging rather than histologic confirmation. Further study is necessary, in which tissues are obtained directly from the brain lesion, revealing the molecular biologic characteristics of the BMs more reliably.

CONCLUSIONS

We demonstrated that there is no correlation between ADC values (ADC_{min} or nADC ratio) of the solid components of the BM from lung cancer and their histologic type. However, the *EGFR* gene mutation status of BM from lung adenocarcinoma can be predicted using ADC values. A further prospective, large-scale cohort study is needed to demonstrate the relationship between gene mutation status and ADC values.

ACKNOWLEDGMENTS

All authors appreciate Heae Surng Park for her assistance in pathologic review of this study.

REFERENCES

1. Nayak L, Lee EQ, Wen PY. **Epidemiology of brain metastases.** *Curr Oncol Rep* 2012;14:48–54 CrossRef Medline
2. Jemal A, Tiwari RC, Murray T, et al; American Cancer Society. **Cancer statistics, 2004.** *CA Cancer J Clin* 2004;54:8–29 CrossRef Medline
3. Shin HR, Ahn YO, Bae JM, et al. **Cancer incidence in Korea.** *Cancer Res Treat* 2002;34:405–08 CrossRef Medline
4. Won YJ, Sung J, Jung KW, et al. **Nationwide cancer incidence in Korea, 2003–2005.** *Cancer Res Treat* 2009;41:122–31 CrossRef Medline
5. Lynch TJ, Bell DW, Sordella R, et al. **Activating mutations in the epidermal growth factor receptor underlying responsiveness of non-small-cell lung cancer to gefitinib.** *N Engl J Med* 2004;350:2129–39 CrossRef Medline
6. Mok TS, Wu YL, Thongprasert S, et al. **Gefitinib or carboplatin-paclitaxel in pulmonary adenocarcinoma.** *N Engl J Med* 2009;361:947–57 CrossRef Medline
7. Johnson ML, Sima CS, Chaft J, et al. **Association of KRAS and EGFR mutations with survival in patients with advanced lung adenocarcinomas.** *Cancer* 2013;119:356–62 CrossRef Medline
8. Eichler AF, Kahle KT, Wang DL, et al. **EGFR mutation status and survival after diagnosis of brain metastasis in nonsmall cell lung cancer.** *Neuro Oncol* 2010;12:1193–99 CrossRef Medline
9. Wieduwilt MJ, Valles F, Issa S, et al. **Immunochemotherapy with intensive consolidation for primary CNS lymphoma: a pilot study and prognostic assessment by diffusion-weighted MRI.** *Cancer Res Treat* 2012;18:1146–55 CrossRef Medline
10. Lee EJ, Lee SK, Agid R, et al. **Preoperative grading of presumptive low-grade astrocytomas on MR imaging: diagnostic value of minimum apparent diffusion coefficient.** *AJNR Am J Neuroradiol* 2008;29:1872–77 CrossRef Medline
11. Guo AC, Cummings TJ, Dash RC, et al. **Lymphomas and high-grade astrocytomas: comparison of water diffusibility and histologic characteristics.** *Radiology* 2002;224:177–83 CrossRef Medline
12. Lee KC, Moffat BA, Schott AF, et al. **Prospective early response im-**

aging biomarker for neoadjuvant breast cancer chemotherapy. *Cancer Res Treat* 2007;13:443–50 Medline
13. Huang WY, Wen JB, Wu G, et al. **Diffusion-weighted imaging for predicting and monitoring primary central nervous system lymphoma treatment response.** *AJNR Am J Neuroradiol* 2016;37: 2010–18 CrossRef Medline
14. Hayashida Y, Hirai T, Morishita S, et al. **Diffusion-weighted imaging of metastatic brain tumors: comparison with histologic type and tumor cellularity.** *AJNR Am J Neuroradiol* 2006;27:1419–25 Medline
15. Duygulu G, Ovali GY, Calli C, et al. **Intracerebral metastasis showing restricted diffusion: correlation with histopathologic findings.** *Eur J Radiol* 2010;74:117–20 CrossRef Medline
16. Han SW, Kim TY, Hwang PG, et al. **Predictive and prognostic impact of epidermal growth factor receptor mutation in non-small-cell lung cancer patients treated with gefitinib.** *J Clin Oncol* 2005;23: 2493–501 CrossRef Medline
17. Cho BC, Im CK, Park MS, et al. **Phase II study of erlotinib in advanced non-small-cell lung cancer after failure of gefitinib.** *J Clin Oncol* 2007;25:2528–33 CrossRef Medline
18. da Cunha Santos G, Shepherd FA, Tsao MS. **EGFR mutations and lung cancer.** *Annu Rev Pathol* 2011;6:49–69 CrossRef Medline
19. Lee YJ, Choi HJ, Kim SK, et al. **Frequent central nervous system failure after clinical benefit with epidermal growth factor receptor tyrosine kinase inhibitors in Korean patients with nonsmall-cell lung cancer.** *Cancer* 2010;116:1336–43 CrossRef Medline
20. Matsumoto S, Takahashi K, Iwakawa R, et al. **Frequent EGFR mutations in brain metastases of lung adenocarcinoma.** *Int J Cancer* 2006; 119:1491–94 CrossRef Medline
21. Omuro AM, Kris MG, Miller VA, et al. **High incidence of disease recurrence in the brain and leptomeninges in patients with nonsmall cell lung carcinoma after response to gefitinib.** *Cancer* 2005;103: 2344–48 CrossRef Medline
22. Gazdar AF. **Activating and resistance mutations of EGFR in non-small-cell lung cancer: role in clinical response to EGFR tyrosine kinase inhibitors.** *Oncogene* 2009;28(suppl 1):S24–31 CrossRef Medline
23. Greulich H, Chen TH, Feng W, et al. **Oncogenic transformation by inhibitor-sensitive and -resistant EGFR mutants.** *PLoS Med* 2005;2: e313 CrossRef Medline
24. Ichihara S, Toyooka S, Fujiwara Y, et al. **The impact of epidermal growth factor receptor gene status on gefitinib-treated Japanese patients with non-small-cell lung cancer.** *Int J Cancer* 2007;120: 1239–47 CrossRef Medline
25. Jackman DM, Yeap BY, Sequist LV, et al. **Exon 19 deletion mutations of epidermal growth factor receptor are associated with prolonged survival in non-small cell lung cancer patients treated with gefitinib or erlotinib.** *Clin Cancer Res* 2006;12:3908–14 CrossRef Medline
26. Carey KD, Garton AJ, Romero MS, et al. **Kinetic analysis of epidermal growth factor receptor somatic mutant proteins shows increased sensitivity to the epidermal growth factor receptor tyrosine kinase inhibitor, erlotinib.** *Cancer Res* 2006;66:8163–71 CrossRef Medline
27. Mulloy R, Ferrand A, Kim Y, et al. **Epidermal growth factor receptor mutants from human lung cancers exhibit enhanced catalytic activity and increased sensitivity to gefitinib.** *Cancer Res* 2007;67: 2325–30 CrossRef Medline
28. Heon S, Yeap BY, Britt GJ, et al. **Development of central nervous system metastases in patients with advanced non-small cell lung cancer and somatic EGFR mutations treated with gefitinib or erlotinib.** *Clin Cancer Res* 2010;16:5873–82 CrossRef Medline
29. Sekine A, Kato T, Hagiwara E, et al. **Metastatic brain tumors from non-small cell lung cancer with EGFR mutations: distinguishing influence of exon 19 deletion on radiographic features.** *Lung Cancer* 2012;77:64–69 CrossRef Medline
30. Takano K, Kinoshita M, Takagaki M, et al. **Different spatial distributions of brain metastases from lung cancer by histological subtype and mutation status of epidermal growth factor receptor.** *Neuro Oncol* 2016;18:716–24 CrossRef Medline
31. Slebos RJ, Kibbelaar RE, Dalesio O, et al. **K-ras oncogene activation as a prognostic marker in adenocarcinoma of the lung.** *N Engl J Med* 1990;323:561–65 CrossRef Medline
32. Soda M, Choi YL, Enomoto M, et al. **Identification of the transforming EML4-ALK fusion gene in non-small-cell lung cancer.** *Nature* 2007;448:561–66 CrossRef Medline
33. Shaw AT, Kim DW, Nakagawa K, et al. **Crizotinib versus chemotherapy in advanced ALK-positive lung cancer.** *N Engl J Med* 2013;368: 2385–94 CrossRef Medline
34. Mak KS, Gainor JF, Niemierko A, et al. **Significance of targeted therapy and genetic alterations in EGFR, ALK, or KRAS on survival in patients with non-small cell lung cancer treated with radiotherapy for brain metastases.** *Neuro Oncol* 2015;17:296–302 CrossRef Medline
35. Jamshidi N, Diehn M, Bredel M, et al. **Illuminating radiogenomic characteristics of glioblastoma multiforme through integration of MR imaging, messenger RNA expression, and DNA copy number variation.** *Radiology* 2014;270:1–2 CrossRef Medline